

Evaluation of the Land Use/Land Cover (LULC) Change Effects on Land Surface Temperature (LST): A Case Study of Kağıthane Watershed

Betül UYGUR ERDOĞAN^{1*}, Reyhan SAĞLAM¹, Rabia Vildan YAR²

¹Istanbul University-Cerrahpasa, Faculty of Forestry, Watershed Management Department, Istanbul, TÜRKİYE

²Istanbul Medipol University, English Language School, Istanbul, TÜRKİYE

*Corresponding Author: uygurb@iuc.edu.tr

Received Date: 20.11.2023

Accepted Date: 08.05.2024

Abstract

Aim of study: This study was carried out to determine the effects of land use/land cover (LULC) change on land surface temperature (LST) using Landsat satellite images.

Area of study: The study area is the Kağıthane watershed in Istanbul, where population growth and LULC changes are experienced most strikingly.

Material and methods: Landsat 5 for 2002 and Landsat 8 for 2021 were used to investigate the relationship between LULC and LST and the correlation between NDVI and LST by the steps of classification of Landsat images to determine the change in LULC, estimation of normalized difference vegetation index (NDVI), calculation of the LST for 2002 and 2021.

Main results: When the results were examined, the major increase and decrease were 1014.7 ha and 933.3 ha in urban and forest areas, respectively. The highest LST values related to LULC were observed in urban and open areas while the lowest values were observed in forest areas and water bodies. Besides, the lowest increase in LST was 0.6°C in forest areas, whereas the highest increase was detected in urban areas with 2.6°C.

Research highlights: This study has shown the importance of protecting the forest areas in the watershed from fragmentation and how necessary it is to plan forests or green areas for cooling the urban climate.

Keywords: Land Use/Land Cover (LULC), Land Surface Temperature (LST), Forest Areas, Urban Watersheds, Cooling Effect

Arazi Kullanımı/Arazi Örtüsü (AKAÖ) Değişiminin Arazi Yüzey Sıcaklığı (AYS) Üzerindeki Etkilerinin Değerlendirilmesi: Kağıthane Havzası Örneği

Öz

Çalışmanın amacı: Bu çalışma Landsat uydu görüntüleri kullanılarak arazi kullanımı/arazi örtüsü (AKAÖ) değişiminin arazi yüzey sıcaklığı (AYS) üzerindeki etkilerini belirlemek ve AYS'de arazi kullanımı olarak orman örtüsü ve kentleşmenin sonuçları arasındaki farkları ortaya koymak amacıyla yapılmıştır.

Çalışma alanı: Nüfus artışı ile arazi kullanımı/arazi örtüsü değişimlerinin en dikkat çekici şekilde yaşandığı İstanbul ilinde yer alan Kağıthane Havzası çalışma alanı olarak seçilmiştir.

Materyal ve yöntem: Bu kapsamda 2002 yılı için Landsat 5 ve 2021 yılı için Landsat 8 uydu görüntüleri kullanılmıştır. Bu veri kaynakları, Kağıthane Havzası için Landsat görüntülerinin arazi kullanımlarına göre sınıflandırılması, normalleştirilmiş bitki örtüsü farkının (NDVI) tahmin edilmesi, 2002-2021 yılları arasında arazi yüzey sıcaklığının belirlenmesi, hesaplama adımları ile AKAÖ ile AYS arasındaki ilişkiyi ve NDVI ile AYS arasındaki korelasyonu araştırmak için kullanıldı.

Temel sonuçlar: Çalışma sonuçları incelendiğinde, 2002-2021 yılları arasında AKAÖ'ye bağlı AYS değerleri en yüksek kentsel ve açık alanlarda gözlenirken; en düşük değerler ise orman alanları ve su yüzeylerinde gözlenmiştir. Bununla birlikte AYS'deki en düşük artış 0.6°C ile orman alanlarında; en yüksek artış da 2.6°C ile kentsel alanlarda tespit edilmiştir.

Araştırma vurguları: Bu çalışma havzadaki orman alanlarının parçalanmadan korunmasının önemini ve kent ikliminde serinletici etkinin artırılabilmesi için de orman alanlarının veya yeşil alanların kent içerisinde planlanmasının yapılmasının ne kadar gerekli olduğunu göstermiştir.

Anahtar Kelimeler: Arazi Kullanımı/Arazi Örtüsü (AKAÖ), Arazi Yüzey Sıcaklığı (AYS), Orman Alanları, Kentsel Havzalar, Serinletme Etkisi



Introduction

The world is getting increasingly urbanized nowadays. It is stated that by 2050, 68% of the world's population will live in cities, while it is foreseen that this rate will increase from 75.1% to 86% in Turkey according to a United Nations report (UN, 2019). As a result, increased population and urban sprawl have become the major components of the land use/land cover (LULC) change in the world. This has led to an increase in the pressure on natural resources and the conversion of land worldwide, as it is in Turkey. Additionally, a growing population means a greater demand from the ecosystems. Therefore, this causes many differences between rural-urban gradients in the context of climate and hydrological properties. Especially, the changes in LULC have critical impacts on some variables such as temperature, humidity, precipitation, albedo, cloudiness, and air pollution, whereas they vary from region to region. At that point, urbanization is the main factor that makes these differences even more severe. Therefore, urbanization has dramatically altered natural and semi-natural surfaces into impermeable urban buildings and disrupted not only the balance of the Earth's surface radiation and energy but also the composition of the atmospheric structure in the near-surface (Foley et al., 2005; Song et al., 2018). Thus, the surface elements of urban areas consist of impervious materials such as concrete, asphalt, and metal creating significant differences in the heat balance in urban areas (Özyuvacı, 1999; Kisthawal, 2010). The replacement of natural land surfaces with artificial surfaces in urban areas leads to the accumulation of solar energy which makes urban air warmer up to 2-10°C than surrounding non-urban areas (Oke, 1988). This difference is called an urban heat island (UHI). However, due to its changing structure, the increase in obstacles against air flows, the contribution of urban and industrial heat sources, biological and industrial wastes, transportation vehicles, and the suspended aerosols in the atmosphere increase, and as a result, air pollution occurs. Although this situation causes the relative humidity to be lower in urban areas, it leads to an increase in the greenhouse effect (Türkeş, 2008). For

instance, Nayak and Mandal (2012) indicated that Western India was getting warmer due to increased greenhouse gas concentration and LULC changes.

In addition, with climate change, the warming of urban areas has gained much more importance and has been the subject of many studies which investigated the relationship between LULC and temperature (Zaeemdar & Baycan, 2017; Yu et al., 2018; Nayak & Mandal, 2019; Ünal et al., 2020; Wahab et al., 2022). Herein, the methods used to reveal the relationship between LULC and temperature used measured air temperature data and determined land surface temperature (LST) according to several thermal remote sensing data. Remote sensing, a highly advanced technology, uses a combination of high-resolution images and image processing tools to effectively reveal changes in land use (Herold et al., 2003; Chaudhuri & Mishra, 2016). With the use of various methodologies, remote sensing has been used for LULC mapping and change analysis (Butt et al., 2015; Liu & Yang, 2015). It has been stated that Landsat satellite images are especially useful for LULC change and also for urbanization (Bagan et al., 2010; Mei et al., 2016). For instance, in the study depending on temperature datasets, Nayak and Mandal (2019) pointed out that India had a warming trend between 1981 and 2006 due to increased dryland and agricultural areas as well as the decrease in shrublands and forested areas. In another study, Karakuş (2019) indicated that urban built-up and bare lands had the highest LST values while the vegetated areas had a lower average LST value which was estimated from Landsat satellite images. Furthermore, Yu et al. (2018) stated that the value of LST increased with an increase in urban areas and also with a decrease in green spaces. Similar results were indicated in the study of Celik et al. (2019) which investigated the relationship between land use/cover changes and land surface temperature in İstanbul. It was mentioned that the mean LST values increased with the expansion of urban areas. Another study which was conducted in Mersin revealed that the transformation of natural areas into artificial areas caused an increase of about 6°C in LST in 28 years (Orhan, 2021). In a study by Ünal et al. (2020) based on

MODIS LST data, the continuous built-up areas, paved roads and a decrease in green areas have been highlighted as the factors causing increased UHI intensity. Additionally, Zaeemdar and Baycan (2017) determined that the most positive exponent relationships were between the artificial surfaces with low albedo, low vegetated areas, and LST depending on Landsat images. Therefore, they noted that this relationship has an increasing effect on UHI formation. Another study based on annual mean air temperature taken from two meteorological stations located in urban and rural areas showed that there was a significant increasing trend in the time series of UHI depending on the substantial modifications in the landscape's surface (Wahab et al., 2022).

These studies show that there is an increasing effect of urban and artificial surfaces on UHI or in contrast, it can be said that there is a negative relationship between green areas and LST which means a cooling effect and was used to mitigate the UHI effects. However, many studies investigated the cooling effect of forests, urban parks, or green spaces (Bowler et al., 2010; Akbari & Kolokotsa, 2016; Moss et al., 2019; Paschalis et al., 2021; Peng et al., 2022). Such that, the construction of green infrastructure and blue networks in cities was highlighted as an important nature-based solution to moderate the UHI effects in the study of Peng et al. (2022). Another study conducted by Paschalis et al. (2021) emphasized that urban forests should be preserved as natural reserves for reducing the UHI effect. Also, in the study of Emecen and Erdem (2019), it was mentioned that urban green areas contribute to cooling the urban climate in Samsun. Therefore, it has been found that green areas help cities adapt to climate change successfully. This could be counted as climate regulation ecosystem service of forests (Sturiale & Scuderi, 2019). Urban green infrastructure makes the environment more resilient in two ways (Brumlop & Finckh, 2011). First, it helps with climate adaptation by increasing ecosystem resilience, such as watershed management and conserving agricultural species' genetic diversity. Second, it is used as carbon storage which aids climate change mitigation. Emissions can be reduced in this

way. However, by constructing roads, bridges, and land misuse, people cause fragmentation and degradation in the ecosystem. As a result, urban areas face extreme weather conditions like floods, heat waves, droughts, and other threats (Demuzere et al., 2014).

In this context, the Kağıthane watershed located in the most populated city, Istanbul, in Turkey has been selected to investigate the impact of LULC on LST. Istanbul has always been accepted to be in a critical location throughout history. This characteristic made it densely migrated. Therefore, it has been the most populated city in Turkey for a long time. Indeed, the proportion of the population in this city increased from 24.2% in 1927 to 93.2% in 2021 (Turkish Statistical Institute [TUIK], 2022). Hence, the urban proportion has been increasing heavily. This leads to a severe decline in natural lands which ends up in UHIs and extreme weather conditions. In addition, Istanbul has faced several climate and hydrology-related issues such as floods due to mis-land use that should be understood well to be resilient. That is why, it is important to investigate the correlation between LST and LULC in this city and the results of this study can be utilized by urban planners in terms of planning cooler cities. So that, the current study's objectives were to: reveal the relationship between LULC and LST using remote sensing techniques; determine the effects of LULC on LST between 2002 and 2021; show the differences between the outcomes of both forest cover and urbanization as a land use on LST; finally discuss why and how forests should be included in urban planning to prevent heat island formation along with mitigating climate change effects or adapting to it. For the region, determining the LST by remote sensing is not new, but highlighting the forest areas in terms of cooling effect is novel.

Material and Methods

Study Area

In this study, a watershed located in Istanbul, where about 16 million people inhabit within a total area of approximately 5400 km², has been selected as the study area. The study area is called Kağıthane watershed which is one of the important watersheds on

the European side of Istanbul (39°-45° N and 41°-45° E) (Figure 1). The watershed has an area of 230.3 km² and drains into the Golden Horn which is the estuary of the Alibey and Kağıthane rivers. The watershed's upland is covered by forests, while the lowland is occupied by residential areas. The average

annual precipitation varies from 800 to 1120 mm. The region's main parent materials are Neogen Belgrad and Carboniferous formations with clay schists and alluvial zones seen locally in various portions of the watershed (Çokoyoğlu, 2008).

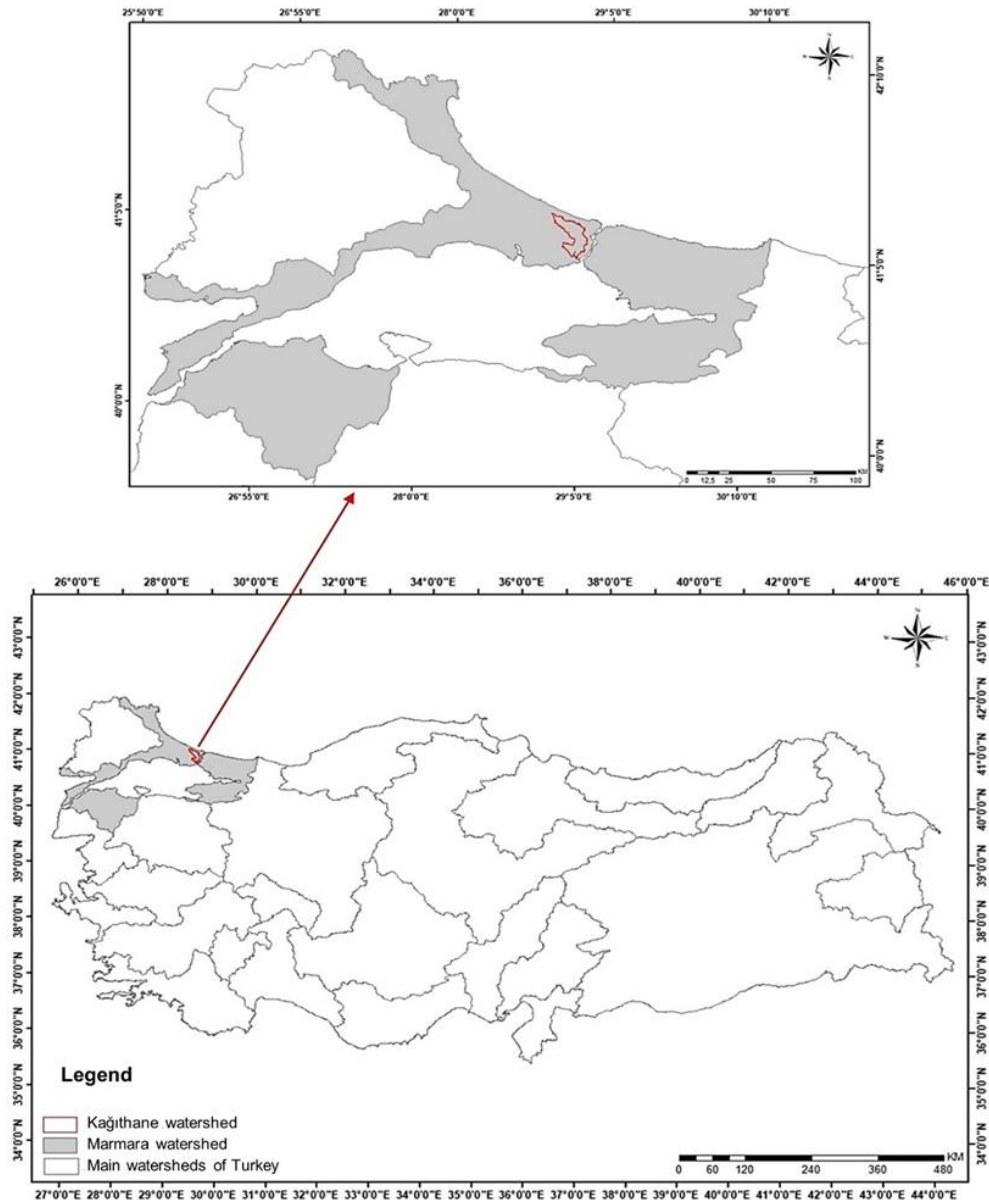


Figure 1. Location of study area

This watershed was selected as the study area because there is a forest within its borders called Belgrad Forest which provides many ecosystem services such as fresh water and recreational facilities to meet the public's demand.

Data Source

In this study, satellite images have been used to investigate the land surface temperature (LST) and the relationship between LULC and LST. The Landsat-5 Thematic Mapper (TM) for 2002; the Landsat-8 (OLI/TIRS) Operational Land

Imager (OLI) for 2021 and Thermal Infrared Sensor (TIRS) were the satellite images intended to be determined. The first Landsat 5 TM image was acquired on July 16, 2002, while the second Landsat 8 OLI image was acquired on August 5, 2021 that covered the study area was downloaded from the United States Geological Survey (USGS) earth explorer website (URL-1, 2022). To avoid seasonal effects, data acquisition time was kept closest for each year in the study by preferring less than 10% cloudiness. ArcGIS 10.1 and Google Earth Pro software were used for the processing, verification, and analysis of satellite images. All of the images and data were converted in the same coordinate system (UTM/WGS 84) to analyze the changes in LULC, normalized difference vegetation index (NDVI), and LST in the study area. All

Landsat images were geometrically rectified to a common map reference system (WGS 84_UTM_zone 35N).

Overall, these data sources were used to investigate the relationship between LULC and LST and the correlation between NDVI and LST by the steps of classification of Landsat images to determine the change in land use and land cover, estimation of normalized difference vegetation index (NDVI), calculation of the land surface temperature (LST) to determine the surface temperature changes in the Kağıthane Watershed due to LULC changes for the years from 2002 to 2021. These steps have been shown as a flowchart of the methodology of this study (Figure 2). These steps were described in the subsequent subsection in detail.

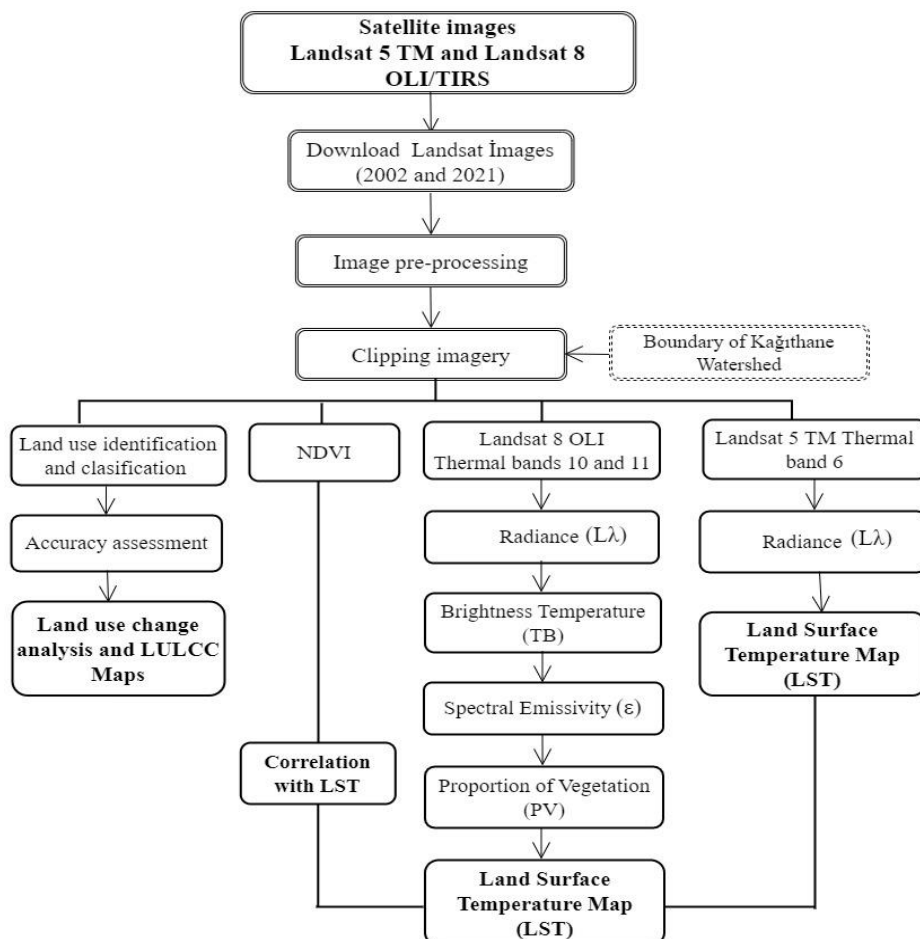


Figure 2. The flowchart of the methodology used in this study

Calculation of Land Surface Temperature

To investigate the LST effect on the central districts of Kağıthane Watershed, the LST

values were calculated using the Landsat thermal images (Band 6 for Landsat 5 TM and Band 10 and Band 11 for Landsat 8 OLI/TIRS

Satellites). The following steps were applied to determine the surface temperature. ArcGIS 10.1 software and its raster calculator tool and map algebra expression were used to assess these steps.

In the first step, Equation 1 was used for Landsat 5 to convert the digital number (DN) of the image to the brightness value, expressed by Ibrahim (2017).

$$L_{\lambda} = (L_{MAX} - L_{MIN})/255 \times DN + L_{MIN} \quad (1)$$

Where:

L_{λ} : Spectral radiance; L_{MAX} : 15.303 (spectral radiance of DN value 255); L_{MIN} : 1.238 (spectral radiance of DN value 1); DN: Digital Number

Equation 2 was used for Landsat 8 (Hashim et al., 2022).

$$L_{\lambda} = M_L \times Q_{cal} + A_L \quad (2)$$

Where:

M_L : Factor scale = 0.0003342; Q_{cal} : DN of band 10 and 11; A_L : Added factor = 0.1

In the second step, the radiance values were converted to the satellite brightness value (°C) using Equation 3 (Hashim et al., 2022).

$$T_B = \frac{K_2}{\ln\left(\frac{K_1}{L_{\lambda}} + 1\right)} - 273.15 \quad (3)$$

Where:

T_B : Effective at-sensor brightness temperature; K_2 : Calibration constant 2 (607.76 for band 6, 1321.0789 for band 10, and 480.8883 for band 11); K_1 : Calibration constant 1 (1260.56 for band 6, 774.8853 for band 10, and 1201.1442 for band 11); \ln : Natural logarithm

In the last step, the temperature was converted from Kelvin to degrees Celsius using Equation 4 (Terfa et al., 2020).

$$LST \text{ (}^{\circ}\text{C)} = \frac{T_B}{\left[1 + \lambda \left(\frac{T_B}{P}\right) \times \ln(\varepsilon)\right]} \quad (4)$$

Where:

T_B : Effective at-sensor brightness temperature; λ : Wavelength of emitted radiance (10.8 μm); P : $(h \cdot c) / k$ (1.438×10^{-2} mk); h : Planck constant (6.626×10^{-34} J s⁻¹); c : velocity of light (2.998×10^8 ms⁻¹); k : Boltzmann constant (1.38×10^{-23} JK⁻¹); ε :

Spectral emissivity value, Using Equation 5 (Hishe et al., 2017).

$$\varepsilon = 0.004 \times P_V + 0.986 \quad (5)$$

Where:

P_V : Proportion of vegetation, calculated with using Equation 6 (Sobrino et al., 2004).

$$PV = \left(\frac{NDVI - NDVI_{min}}{NDVI_{max} - NDVI_{min}}\right)^2 \quad (6)$$

Normalized Difference Vegetation Index (NDVI) Calculation

It is calculated as in equation (7) (Hashim et al., 2022) using the red (R) and near-infrared bands (NIR) of NDVI Landsat satellite images, which are considered to be a good indicator of the surface radiant temperature.

$$NDVI = \frac{NIR - R}{NIR + R} \quad (7)$$

Band 3 with the red band (0.63–0.69 μm) and Band 4 with the infrared band (0.76–0.90 μm) were used in Landsat-5 Thematic Mapper (TM) satellite images. Band 4 with the red band (0.63–0.67 μm) and Band 5 with the infrared band (0.85–0.87 μm) were used in the Landsat-8 OLI/TIRS satellite images (Masek et al., 2020).

Landsat Images Classification

Supervised classification was made on satellite images of 2002 and 2021 to prepare land use land cover change maps. ArcGIS 10.1 software was used to assess the land use change in the Kağıthane Watershed. Many methods are being used to implement supervised classification, such as maximum likelihood, K-nearest neighbor, and minimum distance classification (Muttitanon & Tripathi, 2005). Maximum likelihood algorithm was used to create land use maps. The Maximum likelihood algorithm assigns each spectrally evaluated pixel to the class with the highest correlation (Shalaby & Tateishi, 2007). The classification was made using the best band combination of Landsat satellite images. The maximum likelihood algorithm was applied to classify the LULC of the study area. Considering the interest of the study and dominant LULC, four classes which were forest, urban, bare land, and water body

have been generated based on the current situation. Few other LULC classes can be generated but their proportion is too small and

is not even reflected clearly. For the classification, forty training samples for each class were distributed across the study area.

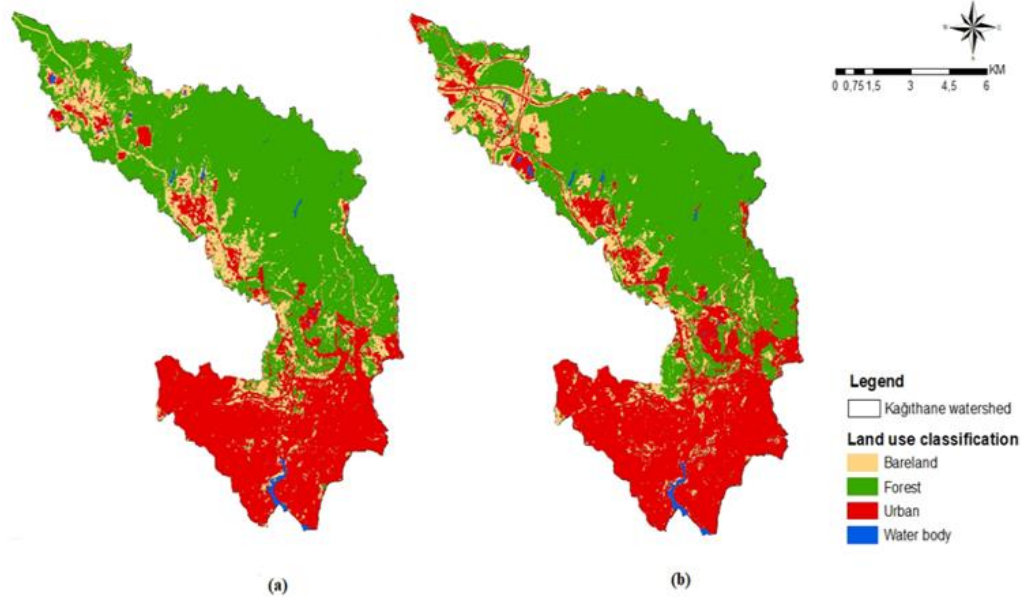


Figure 3. LULC classification for 2002 (a) and 2021 (b) in Kağıthane watershed

On the other hand, classification accuracy assessment plays a critical role in terms of land use mapping and understanding map quality and reliability (Erasu, 2017). Hence, to perform the accuracy assessment, training samples and their representativeness (Lu & Weng, 2007) are essential for image classification. Additionally, developing the error matrix led to obtaining important accuracy assessment metrics such as overall accuracy, producer and user accuracy, and kappa coefficient (Lu & Weng, 2007). So, the accuracy of the classification was calculated using the kappa index besides the overall accuracy, producer, and user accuracy in the current study. To calculate these accuracy assessment components using reference points formed by random sampling method (Wondrade et al., 2014), Google Earth observations were used. Subsequently, accuracy assessment analysis was performed by associating the classification results with the reference points.

Results

LULC Classification

The results of the supervised classification of Landsat images showed the variation in

LULC between 2002 (Figure 3a) and 2021 in the Kağıthane watershed (Figure 3 b). It is clearly seen that the upland of the watershed consists of the forest while the lowland of the watershed is covered by urban areas for both years. Also, the total area of every LULC class and the percentage of these classes were calculated and presented in Table 1.

During the study period, the major increase was observed in urban areas with 1014.7 ha and the major decrease was in forest areas with 933.3 ha. The urban areas were 7492.5 ha in 2002 and 8507.3 ha in 2021 while the forest area was 11244.7 ha in 2021 and 12178.0 ha in 2002. In addition, the size of the bare land also decreased from 3209.2 ha in 2002 to 3112.4 ha in 2021.

In contrast, the area of water bodies increased from 155.1 ha in 2002 to 168.1 ha in 2021 (Table 1). The increase in the size of the water bodies can be attributed to the mine excavation leading to the formation of pit areas in the western north part of the watershed.

Table 1. The area of LULC classes in the Kağıthane watershed for 2002 and 2021

| LULC | 2002 | | 2021 | | Changes in the area (2021-2002) | | |
|------------|-----------|------------|-----------|------------|---------------------------------|------|-------|
| | Area (ha) | Area (%) * | Area (ha) | Area (%) * | (ha) | (%)* | (%)** |
| Bare land | 3209.2 | 13.9 | 3112.4 | 13.5 | -96.8 | -0.4 | -3.0 |
| Forest | 12178.0 | 52.9 | 11244.7 | 48.8 | -933.3 | -4.0 | -7.7 |
| Urban | 7492.5 | 32.5 | 8507.3 | 36.9 | 1014.7 | 4.4 | 13.5 |
| Water body | 155.1 | 0.7 | 168.1 | 0.7 | 13.1 | 0.1 | 8.4 |

*The percentage of each LULC class in a total area of the watershed for the specific years.

**The percent change in the area of each LULC class between specific years.

The comparison of LULC in Kağıthane Watershed revealed that the changes in forest and bare land areas conversely led to an increase in urban areas during the study period (Figure 4).

Furthermore, there are positive changes of 13.5% and 8.4% for urban areas and water bodies respectively, whereas there are negative changes of 7.7% and 3.0% for forest areas and bare land, respectively (Table 1).

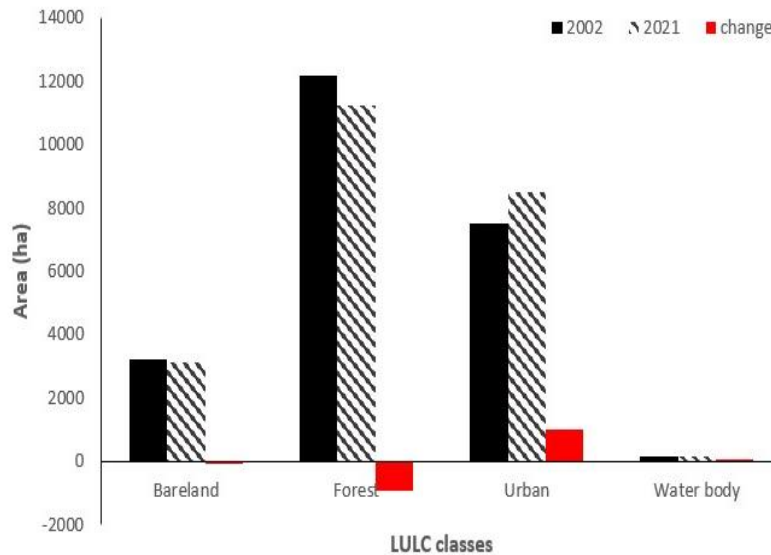


Figure 4. Comparison of LULC and the amount of change in Kağıthane watershed between 2002 and 2021

Accuracy Assessment

When accuracy assessment results were analyzed, the overall accuracy and Kappa coefficient were 95.2% and 0.93, respectively in 2002 (Table 2) and these values were 90.4% and 0.87, respectively in 2021 (Table

3). Wondrade et al. (2014) mentioned that if the kappa coefficients are greater than 0.75 and/or 0.80, the classification and reference data are compatible. The accuracy evaluation results showed that the current study is compatible with the recommended values.

Table 2. Accuracy assessment and Kappa coefficient for LULC in 2002

| LULC | Ground truth/reference | | | | Row total | User accuracy |
|-------------------|------------------------|-------|--------|-----------|-----------|---------------|
| | Water body | Urban | Forest | Bare land | | |
| Water body | 35 | 0 | 0 | 0 | 35 | 100% |
| Urban | 1 | 68 | 2 | 4 | 75 | 90.7% |
| Forest | 0 | 0 | 74 | 1 | 75 | 98.7% |
| Bare land | 0 | 1 | 2 | 42 | 45 | 93.3% |
| Column total | 36 | 69 | 78 | 47 | 230 | |
| Produce accuracy | 97.2% | 98.5% | 94.9% | 89.4% | | |
| Overall accuracy | 95.2% | | | | | |
| Kappa coefficient | 0.93 | | | | | |

Table 3. Accuracy assessment and Kappa coefficient for LULC in 2021

| LULC | Ground truth/reference | | | | Row total | User accuracy |
|-------------------|------------------------|-------|--------|-----------|-----------|---------------|
| | Water body | Urban | Forest | Bare land | | |
| Water body | 34 | 0 | 1 | 0 | 35 | 97.1% |
| Urban | 1 | 62 | 9 | 3 | 75 | 82.7% |
| Forest | 0 | 0 | 73 | 2 | 75 | 97.3% |
| Bare land | 0 | 2 | 4 | 39 | 45 | 86.7% |
| Column total | 35 | 64 | 87 | 44 | 230 | |
| Produce accuracy | 97.1% | 96.9% | 83.9% | 88.6% | | |
| Overall accuracy | 90.4% | | | | | |
| Kappa coefficient | 0.87 | | | | | |

Normalized Difference Vegetation Index (NDVI)

The NDVI values of the Kağıthane watershed were estimated from Landsat images in 2002 (Figure 5a) and 2021 (Figure 5 b). The NDVI values were in the range of -

0.27 and 0.70 in 2002 (Figure 5a) while the values were -0.08 and 0.59 in 2021 (Figure 5b). The north part of the watershed was covered by a dense forest cover and represented by a high NDVI of 0.70 in 2002.

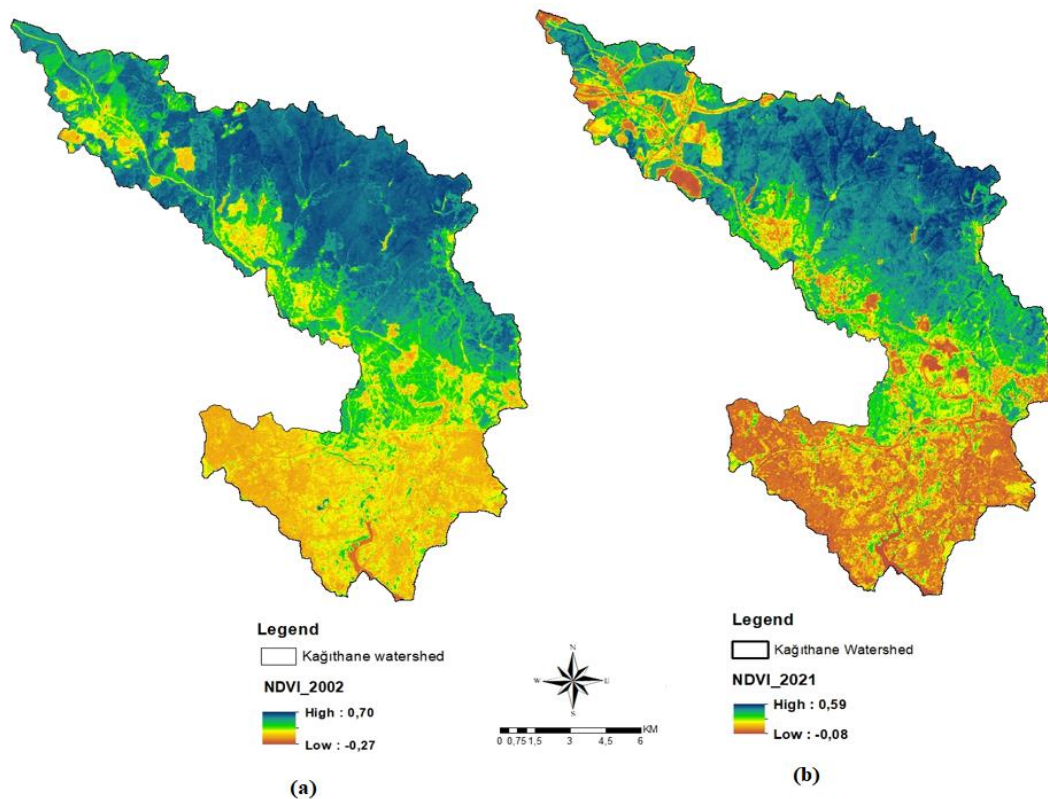


Figure 5. The NDVI values of the Kağıthane watershed estimated from Landsat 5 (a) in 2002 and Landsat 8 (b) in 2021

On the contrary, the south part of the watershed was covered by dense urbanization and represented by the lowest NDVI of -0.27 in 2002. In addition, in 2002, the urban sprawl was developing towards the northern part of the watershed and even some mining fields could be seen in the northwest of the watershed. As a consequence, these areas

were represented by low NDVI values in 2002 (Figure 5 a).

When the NDVI values of the Kağıthane watershed in 2021 were evaluated, it was seen that the northern part of the watershed had a high NDVI value because the area was covered with forests as in 2002. However, the NDVI value for the same area was lower than

in 2002 which was 0.59. However, it was observed that the urbanization in the southern part of the watershed turned into an even more intense structure, and this was reflected in a lower NDVI value compared to 2002. Apart from this, it was observed that the formations in the northwest of the watershed caused fragmentation in the forest areas. Therefore, it can be clearly seen on the map that the NDVI values have been changed for this region as well (Figure 5b).

Land Surface Temperature (LST)

The LST of the Kağıthane watershed was extracted from thermal bands of Landsat

images for July 16, 2002 and August 5, 2021. The LST values ranged between 23.0 and 38.9°C in 2002 as shown in Figure 6a while it ranged between 25.4 and 40.1°C in 2021 as shown in Figure 6 b.

The LST results showed that the northern part of the watershed had low-temperature degrees in both years. In contrast, the southern part of the watershed had high-temperature degrees in both years. Also, the results indicated that the minimum and maximum temperature values of LST were higher (25.4-40.1°C) in 2021 (Figure 6b) than in 2002 (23.0-38.9°C) (Figure 6a).

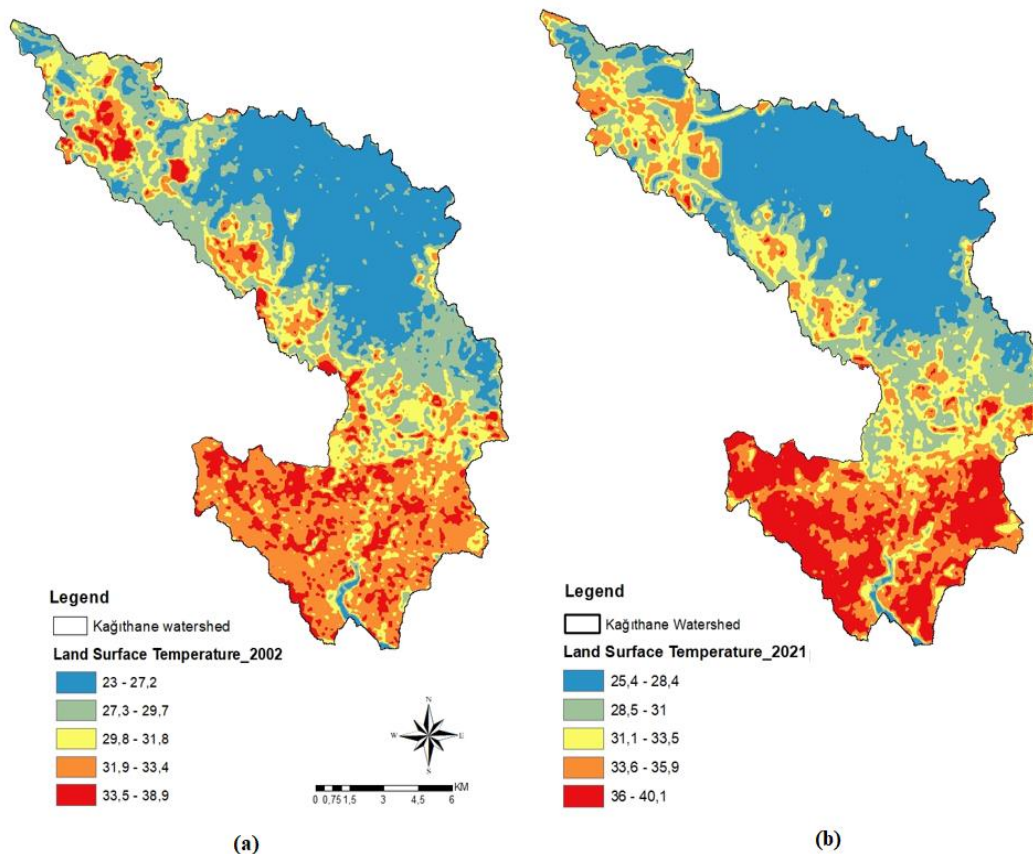


Figure 6. The LST of the Kağıthane watershed estimated from Landsat 5 (a) in 2002 and Landsat 8 (b) in 2021

Additionally, the results of zonal statistics in ArcGIS which describes the relationship between the LST and different LULC classes revealed that urban areas had the highest LST maximum value of 38.9°C and 40.1°C in 2002 and 2021, respectively (Table 4). This was followed by bare lands with a value of 37.7°C in 2002 and 38.9°C in 2021 (Table 4). On the

other hand, the lowest LST value was determined in water with 23.0°C in 2002 and 25.4°C in 2021 (Table 4). Besides water, forestland also had the lowest LST values among the other LULC classes with 26.0°C and 25.7°C in 2002 and 2021, respectively (Table 4). Moreover, when the differences in LST values between 2002 and 2021 were

evaluated, it was observed that the highest increase was in urban areas at 2.6°C, and the

lowest increase was in the forestland at 0.6°C (Table 4).

Table 4. The LST values of different LULC classes in 2002 and 2021

| LULC Class | 2002 | | | | 2021 | | | | Difference (2002-2021) | | |
|------------|------|------|------|-----|------|------|------|-----|------------------------|-----|------|
| | MIN | MAX | MEAN | STD | MIN | MAX | MEAN | STD | MIN | MAX | MEAN |
| Bare Land | 25.6 | 37.7 | 31.2 | 1.8 | 26.7 | 38.9 | 32.6 | 1.8 | 1.1 | 1.2 | 1.3 |
| Forest | 24.7 | 34.2 | 27.5 | 1.6 | 25.7 | 36.9 | 28.1 | 1.5 | 0.9 | 2.7 | 0.6 |
| Urban | 26.0 | 38.9 | 32.6 | 1.1 | 26.5 | 40.1 | 35.1 | 2.2 | 0.5 | 1.2 | 2.6 |
| Water body | 23.0 | 33.0 | 26.6 | 1.7 | 25.4 | 38.8 | 28.7 | 2.0 | 2.4 | 5.8 | 2.1 |

Furthermore, these results showed that LULC significantly affects LST in the Kağıthane watershed. In other words, the LULC variations such as increasing in urban areas or decreasing in forest areas caused an increase in LST in the watershed (Figure 7).

For instance, decreasing of 933.3 ha in the forest area induced an increase in LST from 27.5°C to 28.1°C while increasing of 1014.7 ha in the urban area induced an increase in LST from 32.6°C to 35.1°C in the watershed (Figure 7).

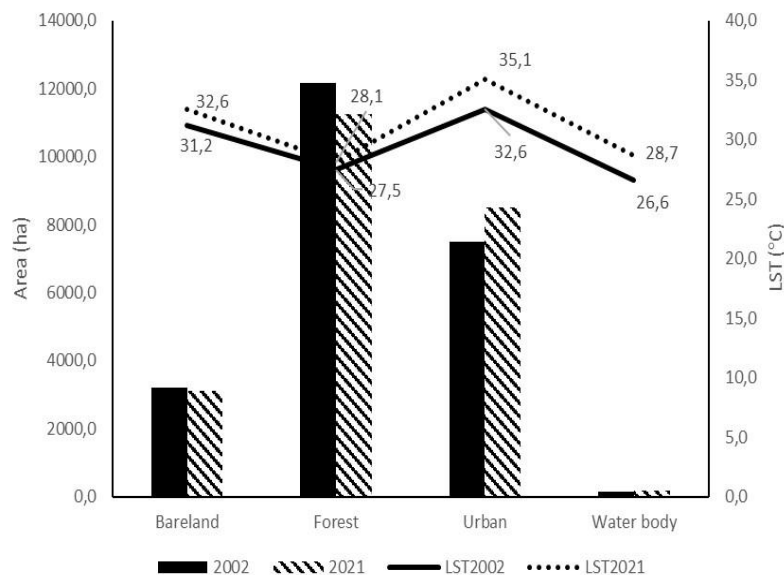


Figure 7. The relation between the LST and LULC of the Kağıthane watershed in 2002 and 2021

Relationship between LST and NDVI

A negative correlation was determined between NDVI values and LST values when a general assessment was made between both parameters in the current study for 2002 and 2021 (Figures 8 and 9). The R² values were observed as 0.75 and 0.79 for the years 2002 and 2021, respectively.

Areas covered by the highest NDVI values are located in the northern part of the watershed. The lowest NDVI values are concentrated in an area covering the urbanized part of the watershed. Areas covered by the highest NDVI values are usually forested areas (Figure 5a and b). NDVI values

increased with the increase of vegetated areas while the LST values decreased.

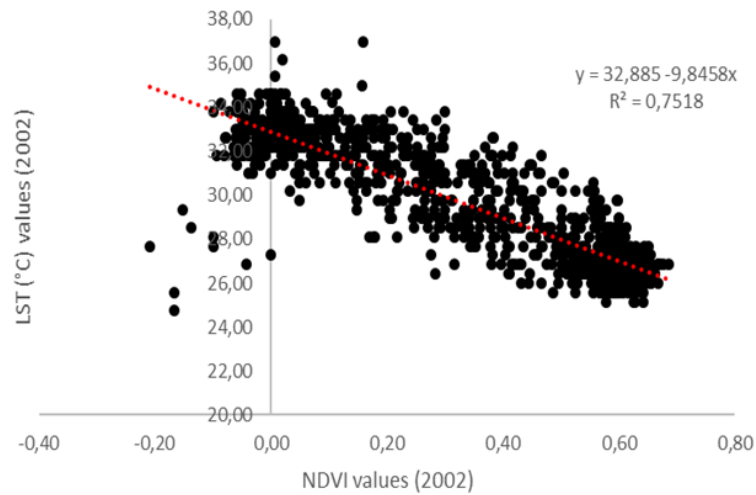


Figure 8. The correlation between NDVI and LST values in 2002

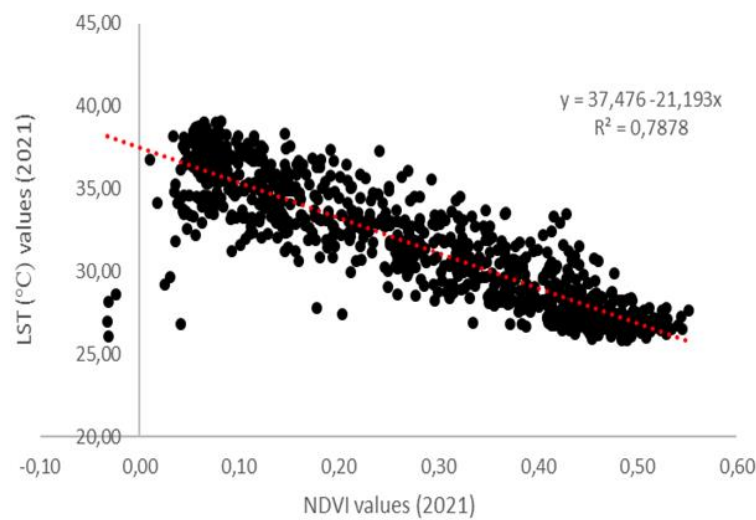


Figure 9. The correlation between NDVI and LST values in 2021

Discussion

The comparison of LST according to the LULC in the Kağıthane watershed was examined in this present study. To gain this purpose, satellite images were used in a lot of research around the world and also in Turkey, for analyzing the relationship between LULC and LST values during a study period (Dihkan et al., 2015; Aslan & Koc-San, 2016; Sarp et al., 2018; Fatami & Narangifard, 2019; Halder et al., 2022; Kaiser et al., 2022).

In this context, the Landsat 5 TM and Landsat 8 OLI were used to evaluate the LULC and LST values in 2002 and 2021, respectively in this study. The results of this the study indicated that the highest LST mean values were estimated in urban areas at 32.6°C and 35.1°C for the years 2002 and 2021,

respectively. The same was also valid for the maximum LST values, and the maximum LST values for both years were the highest in urban areas with 38.9°C and 40.1°C in 2002 and 2021, respectively. These results were consistent with the results of studies conducted worldwide. For instance, Morsy and Morsy & Hadi (2022) indicated that urban cover revealed maximum LST values compared to vegetation and water bodies in Egypt. Also, Halder et al. (2022) determined the changes in LST and LULC and analyzed the relationship between these factors in India. As a result of this study, an increasing trend of LST was observed between 1990 and 2020 due to rapid urbanization, population, and industrialization. Mondal et al. (2021) emphasized that LST values in the city center,

where urbanization is increasing, will increase at an alarming level every 10 years. Additionally, another study conducted in Turkey investigated that the city center has the highest LST value and pointed out that the LST value increased by 4.5°C from rural areas toward the city center (Soydan, 2020). A similar result which was obtained by Okumuş and Terzi (2021) for Istanbul indicated that the surface temperature difference between urban and rural areas reached 4.3°C.

On the other hand, the land use class with high LST values following urban areas was the bare land in this study. The LST value for the bare land varied between 25.6°C and 37.7°C in 2002 whereas it was determined between 26.7°C and 38.9°C in 2021. Also, the LST mean values of bare land were the second highest values for both years of the study period with 31.2°C and 32.6°C values in 2002 and 2021, respectively. A high LST value for bare land was also reported in a previous study with a value of 46.0°C in Baghdad (Hashim et al., 2022). In another study, it has been stated that the construction surfaces (in this study this class is urban) and the open spaces with little or no vegetation class (in this study this class is bare land) trigger heat island formation in the summer months (Kesgin Atak & Ersoy Tonyaloğlu, 2020). Apart from this, an essential detail about bare land is that this land use type is generally exposed to conversion into another land use, especially in urban watersheds. Also, this reduces the area of bare land and affects the LST depending on the converted LULC class as examined in the present study. In addition, if the bare land is converted into urban areas, this may also cause high LST values. However, Fatami and Narangifard (2019) mentioned that the bare lands decreased because of population growth and urbanization.

Despite the high LST values for urban and bare lands, the low LST values were determined for forests and water bodies in the present study. When the LST mean values were examined for the study periods, the water bodies had the lowest LST mean value at 26.6°C in 2002 whereas the forests had the lowest LST mean value at 28.1°C in 2021. In addition, the lowest LST maximum value of 33.0°C was determined for water bodies in 2002, while this was changed to forests as

36.9°C in 2021. In this case, the excavation of mine areas in the western-north part of the watershed verifies the increased area of the water body. Therefore, it can be said that mining processes caused an increment of LST values for water bodies. However, it is not enough to accept that this is the only reason to increase the LST values. The air temperature also becomes important in this phase as it affects the LST values. Therefore, the air temperature has been measured higher than long-term averages in the Marmara region in 2021 (Turkish State Meteorological Service [MGM], 2022).

The lowest LST values for water bodies and forests/vegetated areas were also determined in previous studies (Hashim et al., 2022; Khorrami et al., 2021; Morsy & Hadi, 2022; Kesgin Atak & Ersoy Tonyaloğlu, 2020). This situation can be attributed to high NDVI values of water bodies and forests as it was emphasized in those studies as well. Pandey et al. (2022) found that while vegetation surface and agricultural land generate low LST the settlement and fallow land generate high LST. Moreover, the trees and vegetation have a crucial role in decreasing surface and air temperatures by providing shade and through evapotranspiration (Akbari et al., 1997; Carrillo-Niquete et al., 2022). Similarly, Ellison et al. (2017) mentioned that the climate-cooling effects of the forest should be recognized as the principal contribution of trees against climate change especially for adaptation. Besides, the structure (size, shape, composition, canopy cover, etc.) and the boundary particularly determine the scale of the cooling effect (Bowler et al., 2010). Additionally, a decrease in the quantity of vegetation causes the deterioration of vegetation quality, which was highlighted as the source of augmented LST due to the transformation of vegetation areas into bare lands and urban areas in the study of Fatami and Narangifard (2019). In other words, fragmentation and degradation of forests and green areas also have negative effects on the processes of cooling. In the present study, the northern part of the watershed consisted of forests and as a result of this, the highest NDVI values and lowest LST were investigated in this part of the study area

where the forests have a dense structure that can provide this. However, this part of the study area had been under the pressure of new constructions for highways and mining excavation, and also the area of forests decreased by 933.3 ha in the watershed. Thus, the fragmentation and degradation of forests can be seen in 2002 and 2021 for mining and highway constructions, respectively. Also, this may explain the difference in LST values for the same part of the study area between 2002 and 2021. For instance, Carrillo-Niquete et al. (2022) determined the increase of LST in a range of 2.6-3.9°C after deforestation. Therefore, it can be said that there is a negative relation between the high LST values and vegetation or vice versa. This is also consistent with the negative correlation results between LST and NDVI in the current study. Also, the relationship between NDVI and LST was mentioned as a significant correlation (Kaufmann et al., 2003; Chen et al., 2006), and the increase in LST values was associated with a decrease in NDVI values (Bokaie et al., 2016). In addition Li et al. (2014) stated that vegetated land has a significant and negative relationship with LST. On the other hand, Guha and Govil (2023) found a neutral relationship between LST and NDVI. They emphasized that the reason for this situation is that the earth's surface properties and weather conditions may change during the winter months.

Conclusion

This study examined the effects of LULC change on LST, which were determined for the Kağıthane watershed from 2002 to 2021, using Landsat satellite imagery. When an assessment was made on the obtained results, it was seen that urbanization has an increasing impact on LST in this study. Kağıthane watershed was selected as a case study to analyze the effects of LULC on LST between 2002 and 2021. When the LST values were examined, the mean temperature difference in forest areas increased by 0.6 °C, while this value was the highest value observed in urban areas with an increase of 2.6 °C. Therefore, the study has a critical value in emphasizing the importance of the cooling effect of forest areas in an important metropolitan area like Istanbul within urban planning in the

adaptation and mitigation process to climate change. In the future projections of this highly-populated city, it is necessary to implement a conservative framework for the green areas to take place in the urban ecosystems in terms of both the cooling effect of green areas and the sustainability of other services provided. However, there are some limitations and future scope of the present study. Firstly, the 2000s were not looked at because the cloudiness rate was above 10%. In this respect, more satellite images can be studied with image enhancement techniques. Secondly, data from a sufficient number of meteorological stations representing the Kağıthane Watershed can be used to significantly verify the result. On the other hand, the lack of air temperature in the area was the limitation of the current study. Finally, some other statistical techniques and diagrams can be applied to present these relationships.

Acknowledgments

This study was presented as an oral presentation at the "6th International Eurasian Conference on Biological and Chemical Sciences (EurasianBioChem 2023)" symposium held in Ankara.

Ethics Committee Approval

N/A

Peer-review

Externally peer-reviewed.

Author Contributions

Conceptualization: B.U.E., R.S., V.R.Y.; Investigation: B.U.E., R.S., V.R.Y.; Material and Methodology: B.U.E., R.S.; Supervision: B.U.E.; Visualization: B.U.E., R.S.; Writing Original Draft: B.U.E., R.S.; Writing-review & Editing: B.U.E., R.S., V.R.Y. Other: All authors have read and agreed to the published version of manuscript.

Conflict of Interest

The authors have no conflicts of interest to declare.

Funding

The authors declared that this study has received no financial support.

References

- Akbari, H., D., M., Kurn, Bretz, S. E., & Hanford, J. W. (1997). Peak power and cooling energy savings of shade trees. *Energy and Buildings*, 25, 139-148.
- Akbari, H. & Kolokotsa, D. (2016). Three decades of urban heat islands and mitigation technologies research. *Energy and Buildings*, 133, 834-842.
- Aslan, N. & Koc-San, D. (2016). Analysis of relationship between urban heat island effect and Land use/cover type using Landsat 7 ETM+ and Landsat 8 OLI images. *International Archives of the Photogrammetry, Remote Sensing and Spatial Information Sciences - ISPRS Archives*, 41, (12-19 July 2016), 821-828.
- Bagan, H., Takeuchi, W., Kinoshita, T., Bao, Y. & Yamagata, Y. (2010). Land cover classification and change analysis in the Horqin sandy land from 1975 to 2007. *IEEE Journal of Selected Topics in Applied Earth Observation and Remote Sensing*, 3(2), 168-177.
- Bokaie, M., Zarkesh, M. K., Arasteh, P. D. & Hosseini, A. (2016). Assessment of urban heat island based on the relationship between land surface temperature and land use/ land cover in Tehran. *Sustainable Cities and Society*, 23, 94-104.
- Bowler, D. E., Buyung-Ali, L., Knight, T. M. & Pullin, S. E. (2010). Urban greening to cool towns and cities: A systematic review of the empirical evidence. *Landscape and Urban Planning*, 97, 147-155.
- Brumlop, S. & Finckh, M. R. (2011). *Applications and potentials of marker assisted selection (MAS) in plant breeding: Applications and potentials of smart breeding*. Final report of the F+E project (FKZ 3508890020), On behalf of the Federal Agency for Nature Conservation. Bundesamt für Naturschutz.
- Butt, A., Shabbir, R., Ahmad, S. S. & Aziz, N. (2015). Land use change mapping and analysis using remote sensing and GIS: a case study of Simly watershed, Islamabad, Pakistan. *The Egyptian Journal of Remote Sensing and Space Science*, 18, 251-259.
- Carrillo-Niquete, G. A., Andrade, J. L., Valdez-Lazalde, J. R., Reyes-García, C. & Hernández-Stefanoni, J. L. (2022). Characterizing spatial and temporal deforestation and its effects on surface urban heat islands in a tropical city using Landsat time series. *Landscape and Urban Planning*, 217, 104280.
- Celik, B., Kaya, S., Alganci, U. & Seker, D. Z. (2019). Assessment of the relationship between land use/cover changes and land surface temperatures: A case study of thermal remote sensing. *Fresenius Environmental Bulletin*, 28(2), 541-547.
- Chaudhuri, G. & Mishra, N. B. (2016). Spatio-temporal dynamics of land cover and land surface temperature in Ganges-Brahmaputra delta: a comparative analysis between India and Bangladesh. *Applied Geography*, 68, 68-83.
- Chen, X. L., Zhao, H. M., Li, P. X. & Yin, Z. Y. (2006). Remote sensing image-based analysis of the relationship between urban heat island and land use/ cover changes. *Remote Sensing of Environment*, 104(2), 133-146.
- Çokoyoğlu, S. (2008). *Alibey ve Kağıthane Havzalarında Arazi Kullanımı ve Sorunların 50 Yıllık Değişimi (The change of the land use and problems in Alibey and Kağıthane watersheds in the 50 years)* [Master's thesis, Istanbul University Institute of Science]. 82 pp. [In Turkish]
- Demuzere, M., Orru, K., Heidrich, O., Olazabal, E., Geneletti, D., et al. (2014). Mitigating and adapting to climate change: Multi-functional and multi-scale assessment of green urban infrastructure. *Journal of Environmental Management*, 146, 107-115.
- Dihkan, M., Karsli, F., Guneroglu, A. & Guneroglu, N. (2015). Evaluation of surface urban heat island (SUHI) effect on coastal zone: The case of Istanbul Megacity. *Ocean and Coastal Management*, 118, 309-316.
- Ellison, D., Morris, C. E., Locatelli, B., Sheil, D., Cohen, J., et al. (2017). Trees, forests and water: Cool insights for a hot world. *Global Environmental Change*, 43, 51-61.
- Emecen, Y. & Erdem, N. (2019). Kent iklimi üzerinde yeşil alanların etkileri. [The effects of green areas on urban climate]. *Peyzaj Araştırmaları ve Uygulamaları Dergisi*, 2, 24-30.
- Erasu, D. (2017). Remote sensing-based urban land use/land cover change detection and monitoring. *Journal of Remote Sensing and GIS*, 6, 5.
- Fatami, M. & Narangifard, M. (2019). Monitoring LULC changes and its impact on the LST and NDVI in District 1 of Shiraz City. *Arabian Journal of Geosciences*, 12, 127.
- Foley, J. A., DeFries, R., Asner, G. P., Barford, C., Bonan, G., et al. (2005). Global consequences of land use. *Science*, 309, 570-574.
- Guha, S. & Govil, H. (2023). Evaluating the stability of the relationship between land surface temperature and land use/land cover indices: a case study in Hyderabad city, India. *Geology, Ecology, and Landscapes*, 00(00), 1-13.

- Halder, B., Bandyopadhyay, J., Khedher, K. M., Fai, C. M., Tangang, F., et al. (2022). Delineation of urban expansion influences urban heat islands and natural environment using remote sensing and GIS-based in industrial area. *Environmental Science and Pollution Research*, 48, 73147-73170.
- Hashim, B. M., Al Maliki, A., Sultan, M. A., Shahid, S. & Yaseen, Z. M. (2022). Effect of land use land cover changes on land surface temperature during 1984–2020: A case study of Baghdad city using landsat image. *Natural Hazards*, 112, 1223-1246.
- Herold, M., Goldstein, N. C. & Clarke, K. C. (2003). The spatiotemporal form of urban growth: measurement, analysis and modeling. *Remote Sensing Environment*, 86, 286-302.
- Hishe, S., Lyimo, J. & Bewket, W. (2017). Effects of soil and water conservation on vegetation cover: a remote sensing based study in the Middle Suluh River Basin, Northern Ethiopia. *Environmental Systems Research*, 6(1), 26.
- Ibrahim, G. R. F. (2017). Urban land use land cover changes and their effect on land surface temperature: Case study using Dohuk City in the Kurdistan Region of Iraq. *Climate*, 5(1), 13.
- Karakuş, C. B. (2019). The impact of land use/land cover (LULC) changes on land surface temperature in Sivas city center and its surroundings and assessment of urban heat island. *Asia-Pacific Journal of Atmospheric Sciences*, 55(2), 1-16.
- Kaiser, E. A., Rolim, S. B. A., Grondona, A. E. B., Hackmann, C. L., de Marsillac Linn, R., et al. (2022). Spatiotemporal influences of LULC changes on land surface temperature in rapid urbanization area through Landsat-TM and TIRS Images. *Atmosphere*, 13(3), 460.
- Kaufmann, R. K., Zhou, L., Myneni, R. B., Tucker, C. J., Slayback, D., et al. (2003). The effect of vegetation on surface temperature: a statistical analysis of NDVI and climate data. *Geophysical Research Letter*, 30(22), 2137.
- Kesgin Atak, B. & Ersoy Tonyaloğlu, E. (2020). Alan kullanım/arazi örtüsü ve bitki örtüsündeki değişimin arazi yüzey sıcaklığına etkisinin değerlendirilmesi: Aydın ili örneği [Evaluation of the effect of land use / land cover and vegetation cover change on land surface temperature: The case of Aydın province]. *Turkish Journal of Forestry*, 21(4), 489-497.
- Khorrami, B., Heidarlou, H. B. & Feizizadeh, B. (2021). Evaluation of the environmental impacts of urbanization from the viewpoint of increased skin temperatures: a case study from Istanbul, Turkey. *Applied Geomatics*, 13, 311-324.
- Kisthawal, C. M., Niyogi, D., Tewari, M., Pielke Sr, R. A. & Shepherd, J. M. (2010). Urbanization signature in the observed heavy rainfall climatology over India. *International Journal of Climatology*, 30(13), 1908-1916.
- Liu, Y., Huang, X., Yang, H. & Zhong, T. (2014). Environmental effects of landuse/ cover change caused by urbanization and policies in Southwest China karst area-a case study of Guiyang. *Habitat International*, 44, 339-348.
- Liu, T. & Yang, X. (2015). Monitoring land changes in an urban area using satellite imagery, GIS and landscape metrics. *Applied Geography*, 56, 42-54.
- Lu, D. & Weng, Q. (2007). A survey of image classification methods and techniques for improving classification performance. *International Journal of Remote Sensing*, 28, 823-870.
- Masek, J. G., Wulder, M. A., Markham, B., McCorkel, J., Crawford, C. J., et al. (2020). Landsat 9: Empowering open science and applications through continuity. *Remote Sensing of Environment*, 248, Article 111968.
- Mei, A., Manzo, C., Fontinovo, G., Bassani, C., Allegrini, A., et al. (2016). Assessment of land cover changes in Lampedusa Island (Italy) using Landsat TM and OLI data. *Journal of African Earth Sciences*, 122, 15-24.
- Mondal, A., Guha, S. & Kundu, S. (2021). Dynamic status of land surface temperature and spectral indices in Imphal city, India from 1991 to 2021. *Geomatics, Natural Hazards and Risk*, 12(1), 3265-3286.
- Moss, J. L., Doick, K. J., Smith, S. & Shahrestani, M. (2019). Influence of evaporative cooling by urban forests on cooling demand in cities. *Urban Forestry and Urban Greening*, 37, 65-73.
- Muttitanon, W. & Tripathi, N. K. (2005). Land use/land cover changes in the coastal zone of Ban Don Bay, Thailand using Landsat 5 TM data. *International Journal of Remote Sensing*, 26(11), 2311-23.
- Morsy, S. & Hadi, M. (2022). Impact of land use/land cover on land surface temperature and its relationship with spectral indices in Dakahlia Governorate, Egypt. *International Journal of Engineering and Geosciences*, 7(3), 272-282.
- Nayak, S. & Mandal, M. (2012). Impact of land-use and land-cover changes on temperature trends over Western India. *Current Science*, 102(8), 1166-1173.
- Nayak, S. & Mandal, M. (2019). Impact of land use and land cover changes on temperature trends over India. *Land Use Policy*, 89, Article 104238.

- Oke, T. (1988). The urban energy balance. *Progress in Physical Geography*, 12, 471-508.
- Okumuş, D. E. & Terzi, F. (2021). Evaluating the role of urban fabric on surface urban heat island: The case of Istanbul. *Sustainable Cities and Society*, 73, Article 103128.
- Orhan, O. (2021). Mersin ilindeki kentsel büyümenin yer yüzey sıcaklığı üzerine etkisinin araştırılması. [Investigation of the effect of urban expansion on surface temperature in Mersin city]. *Journal of Geomatics*, 6(1), 69-76.
- Özyuvacı, N. (1999). *Meteorology and Climatology*. Istanbul University Press No:4196, Istanbul.
- Pandey, A., Mondal, A., Guha, S., Upadhyay, P. K. & Singh, D. (2022). Land use status and its impact on land surface temperature in Imphal city, India. *Geology, Ecology, and Landscapes*, 00(00), 1-15.
- Paschalis, A., Chakraborty, T. C., Faticchi, S., Meili, N. & Manoli, G. (2021). Urban forests as main regulator of the evaporative cooling effect in cities. *AGU Advances*, 2(2), e2020AV000303.
- Peng, J., Cheng, X., Hu, Y. & Corcoran, J. (2022). A landscape connectivity approach to mitigating the urban heat island effect. *Landscape Ecology*, 37, 1707-1719.
- Sarp, G., Temurcin, K. & Aldırmaz, Y. (2018). Evaluation of industrialization effects on urbanization and heat island formation using remote sensing technologies: A case of Istanbul Bağcılar district. *SDU Faculty of Arts and Sciences Journal of Social Sciences*, 44, 1-13.
- Shalaby, A. & Tateishi, R. (2007). Remote sensing and GIS for mapping and monitoring land cover and land-use changes in the Northwestern coastal zone of Egypt. *Applied Geography*, 27(1), 28-41.
- Sobrino, J. A., Jiménez-Muñoz, J. C. & Paolini, L. (2004). Land surface temperature retrieval from LANDSAT TM 5. *Remote Sensing of Environment*, 90(4), 434-440.
- Song, X. P., Hansen, M. C., Stehman, S. V., Potapov, P. V., Tyukavina, A., et al. (2018). Global land change from 1982 to 2016. *Nature*, 560 (7720), 639-643.
- Soydan, O. (2020). Effects of landscape composition and patterns on land surface temperature: Urban heat island case study for Nigde, Turkey. *Urban Climate*, 34(12), 100688.
- Sturiale, L. & Scuderi, A. (2019). The role of green infrastructures in urban planning for climate change adaptation. *Climate*, 7(10), 119.
- Terfa, B. K., Chen, N., Zhang, X. & Niyogi, D. (2020). Spatial configuration and extent explains the urban heat mitigation potential due to green spaces: Analysis over Addis Ababa, Ethiopia. *Remote Sensing*, 12(18), 1-24.
- Turkish State Meteorological Service (MGM, 2022). Climate Assessment for 2021. Ankara, Turkey: MGM.
- Turkish Statistical Institute (TUIK, 2022). Retrieved June 28th 2022 from <https://data.tuik.gov.tr>
- Türkeş, M. (2008). Küresel iklim değişikliği nedir? Temel kavramlar, nedenleri, gözlenen ve öngörülen değişiklikler. *İklim Değişikliği ve Çevre*, 1(1), 26-37.
- United Nations (UN, 2019). Department of Economic and Social Affairs, Population Division. World Urbanization Prospects: The 2018 Revision (ST/ESA/SER.A/420). New York: United Nations.
- URL-1. (2022). United States Geological Survey. What are the band designations for the Landsat satellites?|U.S. Geological Survey (usgs.gov)? Landsat missions. Landsat 8|U.S. Geological Survey (usgs.gov) Landsat 5|U.S. Geological Survey (usgs.gov). www.earthexplorer.usgs.gov.
- Ünal, Y. S., Sonuç, C. Y., Incecik, S., Topcu, H. S., Diren-Üstün, D. H., et al. (2020). Investigating urban heat island intensity in Istanbul. *Theoretical and Applied Climatology*, 139, 175-190.
- Wahab, B. I., Naif, S. S. & Al-Jiboori, M. H. (2022). Development of annual urban heat island in Baghdad under climate change. *Journal of Environmental Engineering and Landscape Management*, 30(1), 179-187.
- Wondrade, N., Dick, Q. B. & Tveite, H. (2014). GIS based mapping of land cover changes utilizing multi-temporal remotely sensed image data in Lake Hawassa watershed, Ethiopia. *Environmental Monitoring and Assessment*, 186(3), 1765-1780.
- Yu, Z., Guo, X., Zeng, Y., Koga, M. & Vejre, H. (2018). Variations in land surface temperature and cooling efficiency of green space in rapid urbanization: The case of Fuzhou city, China. *Urban Forestry & Urban Greening*, 29, 113-121.
- Zaeemdar, S. & Baycan, T. (2017). Analysis of the relationship between urban heat island and land cover in Istanbul through Landsat 8 OLI. *Journal of Earth Science and Climatic Change*, 8, 423.